Effect of Specimen Thickness on Plastic Zone

S. K. Kudari[1a], K. G. Kodancha[2b]

[1]Professor, Department of Mechanical Engineering, B.V.B. College of Engineering and Technology, HUBLI – 580 031, India

[2]Research Scholar, Department of Mechanical Engineering, B.V.B. College of Engineering and Technology, HUBLI – 580 031, India

[a]skkudari@bvb.edu, [b]krishnaraja@bvb.edu

Keywords: crack-tip constraint, finite element analysis, thickness effect, 3D plastic zone size

Abstract. The studies on crack-tip plastic zones are of fundamental importance in describing the process of failure and in formulating various fracture criteria. The study of out-of-plane constraint in fracture analysis is important and needs a detailed 3 dimensional analysis of crack-tip plastic zone. This paper presents 3 dimensional finite element analyses of crack-tip plastic zones and effect of specimen thickness on crack-tip plastic zone shape and size considering a CT specimen with crack length to width ratio (a/W) equal to 0.5. The results indicate that the shape of plastic zone does not correspond to classical "*dog-bone*" shape. The analysis also indicates that the shape of plane stress plastic zone on the specimen surface as expected in classical model is not reproduced. The maximum plastic zone size is found to occur at the centre of the specimen, in contrary to conventional shape, indicating a significant change in the shape of plastic zone. The results are used to discuss the out-of-plane constraint in fracture and specimen size restriction of ASTM J_{IC} fracture test.

Introduction

It is well known that a sharp crack in a loaded machine /structural component made of elastic-plastic material cause development of high stresses and locally yields the material referred as *plastic zone*. Due to the formation of plastic zone the plastic strains in the vicinity of the crack-tip are restrained creating a tri-axial stress-state to occur. This effect is referred as *crack-tip constraint* [1]. The magnitude of constraint depends on the crack-length, the loading type, the component size and geometry. Yuan and Brocks [2] have also considered that constraint literally is a structural obstacle against plastic deformation, which is induced mainly by geometrical and physical boundary conditions. With detailed finite element analysis they have discussed that constraint effects in a specimen depend on the *plastic zone size*. The systematic understanding of crack-tip constraint requires a detailed study of crack-tip plastic deformation in 3 dimensions (3D) to distinguish between *in-plane constraint* and the *out-of-plane constraint* [2]. The in-plane constraint is influenced by specimen dimensions in direction of growing crack (length of the uncracked ligament and the loading conditions). The out-of-plane constraint is influenced by the specimen dimensions parallel to the crack front (specimen thickness). Several parameters, like T-stress [3] and Q-factor [4] are introduced to quantify the in-plane crack-tip constraints, which are more suitable for 2D fracture analysis. But in reality, 3D crack-front fields are significantly affected by out-of-plane stress state, which is difficult to characterize with T and Q parameters [1]. In 3D fracture analysis, constraint effects can be studied by crack-tip plastic zone size. For a given configuration, the plane strain state describes highest possible out-of-plane constraint and generates the highest possible stress triaxility, where as the plane stress yields the lower limit. Since, the fracture test specimens are designed (minimum size requirements) for the maximum crack-tip constraint, neglecting the constraint effects often results in the over-conservative failure predictions by fracture tests. Hence, it

is necessary to explore constraint effects in a fracture specimen by studying the size and shape of crack-tip plastic zone in 3D.

According to the conventional concept, the crack tip plastic zone along the crack front across the thickness of the specimen is given by the so called "*dog-bone*" model as shown in Fig.1. This model assumes a state of plane strain at the centre of the specimen and a state of plane stress on the surface of the specimen [5]. In order to understand the theoretical variation of plastic zone size from surface to center of the specimen, 3D finite element analyses are required. In literature, recently it is found that 3D plastic zone FE models have been studied by Fernandez *et al*. [5] and Herrea *et al*. [6]. But the detailed analysis of plastic zone shape and its size, on the surface and at the centre of the specimen and comparison with the 2D plane stress and plane strain results are lacking. An attempt has been thus directed in this investigation to achieve finite element (FE) estimations of 3D plastic zone shape and size. Primarily, these estimations have been made on Compact Tensile (CT) specimens having different plate thickness. The major objective of this investigation is to elucidate the difference in the plastic zone size at the center and the surface of specimens having various thicknesses by Finite Element (FE) computations, which can address out-of-plane constraint issue in fracture. The results can also be used to address the specimen size requirements of a J_{IC} test [7].

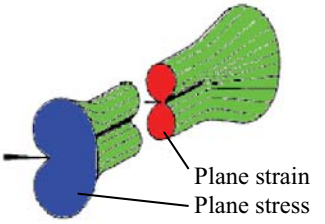

Fig.1 Classical *dog-bone* model of 3D plastic zone shape.

Finite Element Analyses

The entire work has been carried out using commercial finite element code ABAQUS [8]. A series of elastic-plastic stress analyses by finite element method have been carried out on Compact Tensile (CT) specimen, the geometry of the specimen used in the analysis is shown in Fig.2. Due to the symmetry of the specimens under Mode-I loading, only one half of the specimen has been considered in the present 3D FE analysis. The analysis domain is descritized using 20-noded quadratic brick finite elements using reduced integration. This kind of elements is used in the work of Kim *et al.* [9], Courtin *et al.* [10]. The number of elements used for meshing the analysis domain varied with the thickness of the specimen. A typical mesh used in the analysis for thickness B=4 mm is shown in Fig.3.

The 3D shape and size of plastic zone, stress distribution and the magnitude of J-integral were computed by ABAQUS post processor. The effect of specimen thickness on plastic zone (PZ) has been studied by varying the specimen thickness, B= 2, 4, 6, 8, 10 mm (B/W=0.1-0.5, where B-thickness and W-width of the specimen) and applied stress (σ) keeping constant a/W=0.5 (a- crack length). The boundary separating the plastic enclave from the elastic bulk was obtained by iso-stress surface of the effective stress using von Mises yield criterion [11]. In these calculations, the material considered is an interstitial free (IF) steel possessing yield strength (σ_y) of 155 MPa and elastic modulus (E) of 197 GPa [12]. In these calculations, the material response has been considered to be multilinear kinematic hardening type. The material response in plastic deformation was modeled by taking twenty divisions of plastic portion of true stress-true strain curve of the material [11].

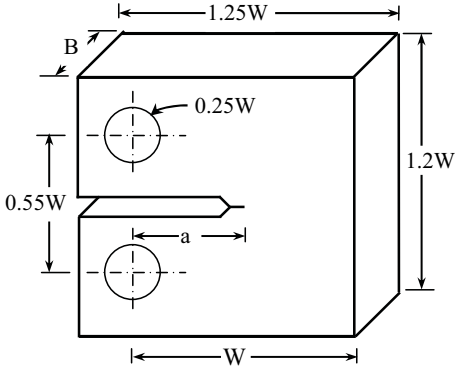

Fig.2 The geometry of CT specimen used in the analysis (W=20 mm).

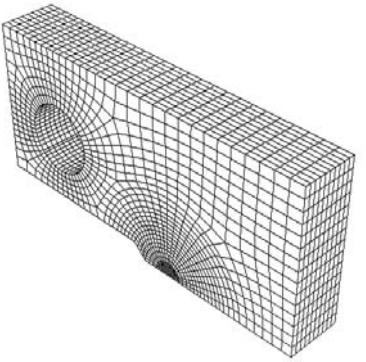

Fig.3 A typical mesh used in the FE analysis for thickness B=4 mm

Results and Discussion

A series of 3D FE stress analyses have been carried out on CT specimen with a/W =0.5 and varied thickness, and applied stress (σ/σ_y=0 -0.75) to study the variation of plastic zone and magnitude of J-integral along the crack-front. The applied stress (σ) in the analysis is computed with the analytical formulation provided in the work of Priest [13]. The details of computation of 3D J-integral are discussed elsewhere [14]. A typical variation of magnitudes of J-integral (for σ/σ_y=0.29 and 0.75) for various specimen thickness is shown in the Fig.4.

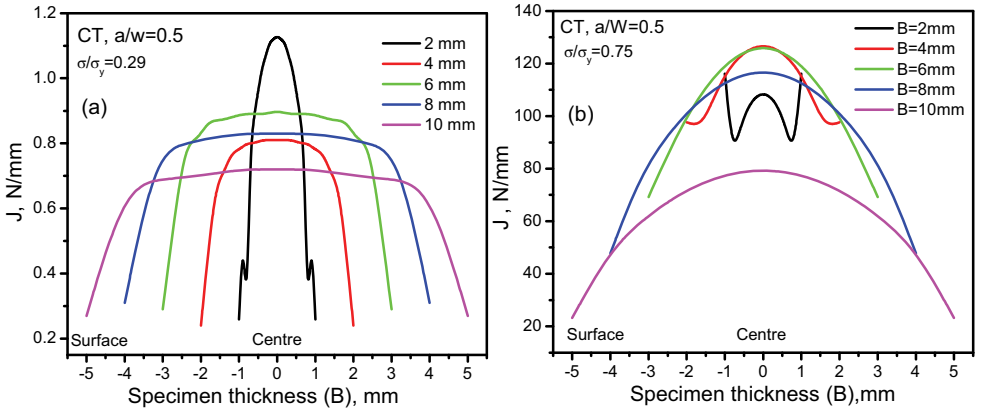

Fig.4 A typical variation of magnitudes of J-integral (a) σ/σ_y =0.29 and (b) σ/σ_y = 0.75 for various specimen thickness considered in the analysis.

This figure indicates that the magnitude of J varies from surface to the centre of the specimen along the crack front. The magnitude of the J is observed to be higher at the centre of the specimen than that of surface. It is also seen from Fig.4 (a) and Fig.4 (b) that the nature variation of J along the crack front is dependent on the applied loading. The variation of the magnitude of J presented in Fig.4 is in similar agreement with the results presented in the work of Zadeh *et al* [15] and Rajaram *et al* [16]. The average value of J (J_{av}) for all specimens having varying thickness is computed and is considered in the analysis.

A typical sequential development of 3D elastic-plastic boundaries in specimens having thickness B=4mm (pertaining to B/W= 0.2) for various applied loads, σ/σ_y =0.319-0.582 (J=0.983- 23.557 N/mm) obtained using elastic-plastic FE analysis are shown in Fig.5. This figure shows that at lower applied load (J_{av}) the shape of plastic zone is similar throughout the thickness from surface to the centre of the specimen. As the load (J_{av}) increases, it is observed that the plastic zone grows more rapidly at the centre than the surface of the specimen. This nature of variation of plastic zone on surface and at the centre is good agreement with the results of Yuan and Brokes [2] and Roychoudhary and Dodds [17]. Further increase in the magnitude of J_{av} results in the growth of PZ on the surface similar to that in the centre of the specimen assuming state of plane stress. These results contradict the theoretically assumed shape of 3D plastic zone shown in Fig.1. The "dog-bone" shape (Fig.1) is verified with 2D FE-results for the considered CT-specimen. It is interestingly found that the 2D plane stress and plane strain PZ shapes obtained by elastic FEA agree well with the limit states of the "dog-bone" model. But the 2D plane stress and plane strain PZ shapes obtained by elastic-plastic FEA do not agree with the "dog-bone" model (Fig.1). The obtained 3D elastic-plastic PZ shapes for specimens of various thicknesses and various applied loads however, show the following discrepancies in comparison to 2D plane stress and plane strain limit states:

For the specimen having B=2mm, the crack tip plastic zones at the surface and at the centre are practically identical to those for the state of plane stress for all applied loads. For the specimen having B>2mm, the crack tip plastic zones are similar in shape on the surface and at the centre only at very low applied load. But at higher magnitudes of J_{av} the PZS at the centre of the specimen grows larger than the PZS on surface showing the condition of plane stress state in contrary to plane strain state assumed in "dog bone" model shown in Fig.1. The results shown in Fig.5 also indicate that the state of stress at the free surface of the specimen gets changed depending on applied load (J_{av}) and is not represented by a state of a plane stress anymore. The smaller size of the crack tip PZS on the surface may be attributed to state of stress on the specimen surface and the lower magnitude of load intensity, J, as depicted in Fig. 4. The varied PZ shape and size ahead of a crack-tip depicted in Fig.5 may be attributed to 3D stress field the varied out-of-plane constraint in the specimen.

The extent of plastic zone size (PZS), r_p, at $\theta=0^o$ (along the ligament) on the surface and at the centre of the specimen have been estimated for a large number of plastic enclaves as typically shown in Fig.5. The outputs of the plastic enclaves obtained by the FE analyses were used to estimate the value of r_p. The magnitude of r_p has been estimated using ABAQUS post processor by making displacement scaling equal to zero and measuring the distance between crack-tip point and the effective stress contour ahead of crack-tip possessing a value equal to the uniaxial yield strength of a material. The magnitude of PZS on the surface and at the centre of the specimen has been computed by slicing the specimen at the centre. A typically sliced specimen at the centre, showing the clear PZS at the surface and at the centre is shown in Fig.6. The results of the extent of plastic zones were compiled as its normalized plastic zone size (r_p/a) *vs*. normalized J- integral ($J/a\sigma_y$) for various specimen thickness (B=2, 4, 6, 8 and 10 mm) obtained using elastic-plastic FE analysis are shown in Fig.7 (a) to Fig. 7(e) respectively. The 2D plane stress and plane strain results of PZS computed using CT specimen are also plotted in the Fig.7 (a) to Fig. 7(e) for comparative assessment with 3D results of PZS. These figures indicate that for specimen with B=2 mm the PZS on surface and at the centre are similar for all applied J_{av}, and these results of PZS also match with the 2D plane stress FE results of PZS. As thickness of the specimen is increased to 4, 6, 8 and 10 mm, it is observed that the PZS is similar on surface and at the centre for only vanishingly small value of normalized J_{av}. The magnitude of normalized J_{av} for which PZS is similar on the surface

and at the centre is dependent on the specimen thickness. Further increase in normalized J_{av} shows a discrepancy in magnitudes of PZS on the surface and at the centre, for all specimen having thicknesses, B >2 mm (ref. Fig.7). The magnitude of PZS is observed to be higher in the centre than the surface of the specimen.

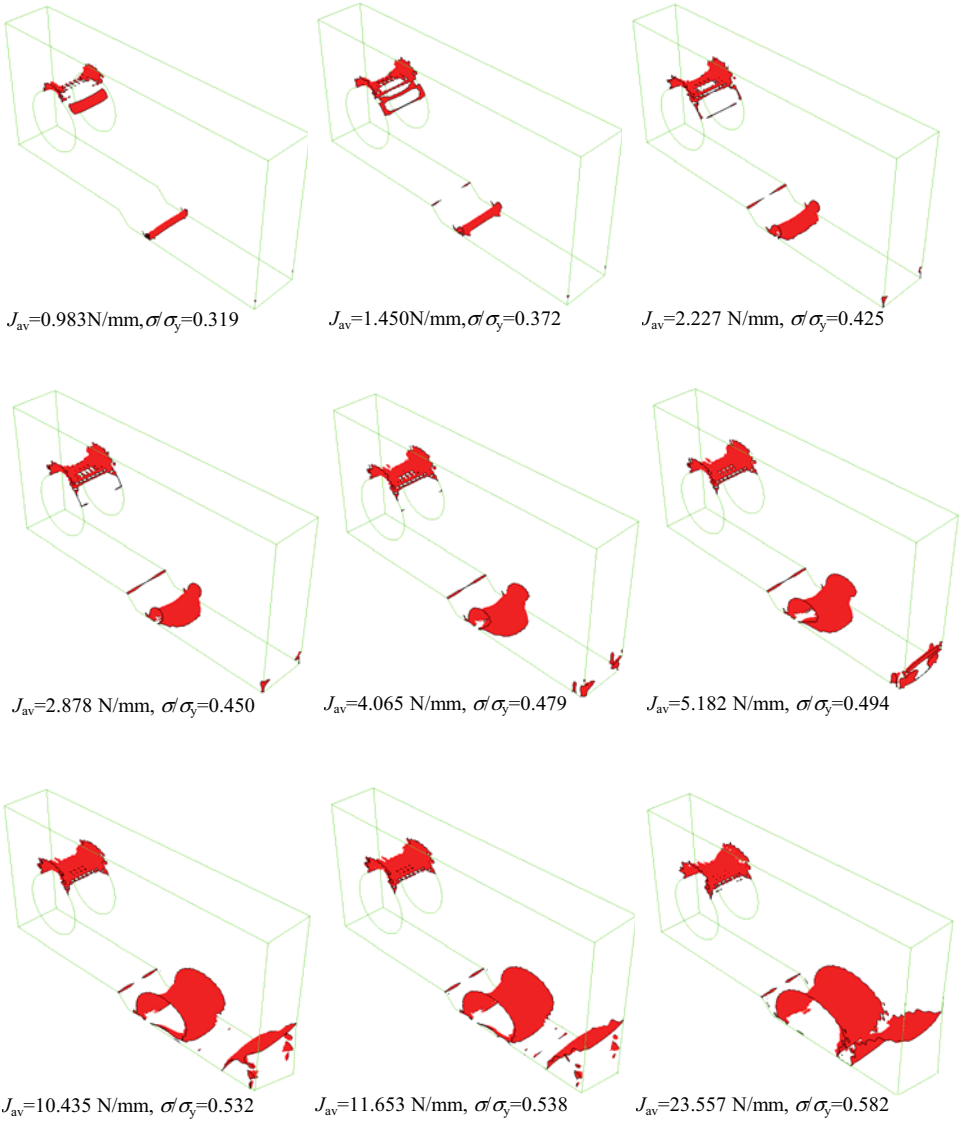

Fig.5 A typical sequential development of 3D elastic-plastic boundaries in specimens having thickness B= 4 mm.

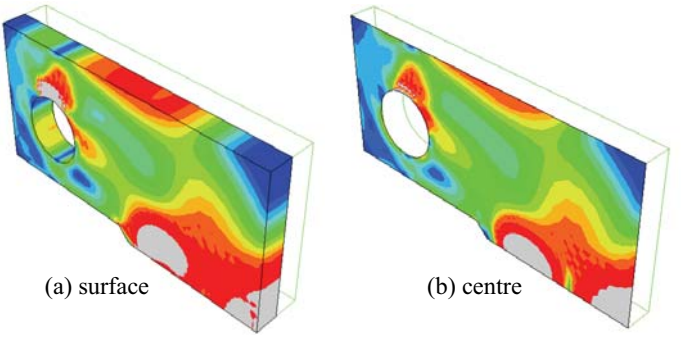

Fig.6 A typical sliced specimen at the centre, showing the clear PZS (a) on the surface and (b) at the centre.

The 3D results on PZS as shown in Fig.5 and Fig.7 demonstrate that: (a) plane stress conditions exist at the crack-tip for specimens with $B/W \leq 0.1$ (b) as thickness of the specimen increases to $B/W \geq 0.1$, plane strain crack-tip condition as expected is not observed, (c) the 3D crack-tip fields locate between plane strain and plane stress states possibly due to more complex 3D crack-tip fields than the 2D stress fields. The complex crack-tip fields in 3D between plane strain and plane stress states may be due to mixing of in-plane and out-of-plane constraints. Hence, the results infer that 3D analysis can not be controlled by a parameter defined under plane strain condition only.

Figure.7 also indicates that the 2D plane strain results of r_p/a are apparently comparable to the 3D results only for limited lower magnitude of normalized J_{av}. At higher normalized J_{av} the 3D results of r_p/a are not comparable to 2D plane strain results even for a specimen with thickness B=10 mm (B/W=0.5), which is the specimen size requirement for valid K_{IC} test [18]. This infers that for specimen thickness B/W=0.5 the plane strain state as expected in the specimen is not achieved; instead specimen shows a mixed plane strain and plane stress state. Therefore, studying out-of plane constraint is a complex issue. Though it is a complex issue, study of out-of plane constraint is important aspect in deciding the minimum specimen size requirement of a J_{IC} fracture test specimen. For valid plane strain J_{IC} fracture test the size requirement of a specimen according to ASTM standard [7] is:

$$B, (W - a) = 25 \frac{J_{IC}}{\sigma_y} \tag{1}$$

where J_{IC} is the plane strain fracture toughness, σ_y is the yield stress of the material. It is well known that the above equation yields the specimen size requirement that is much less than the one used for K_{IC} fracture test [18]. But, when we observe the results presented in the Fig.7, it is clear that even for the specimen with normalized thickness B/W=0.5 (requirement of K_{IC} test) is not satisfying the plane strain condition (As 2D plane strain PZS do not match with 3D PZS). This results infer that the plane strain fracture test done using the specimen restrictions as shown in Eqn.(1) do not seems to satisfy the size requirement of J_{IC} test and can lead to un accountable constraint loss in the CT specimen. Hence, the results obtained in this investigation show a possible need of some modification with respect to the minimum size requirement of J_{IC} test specimen, which is free from constraint loss.

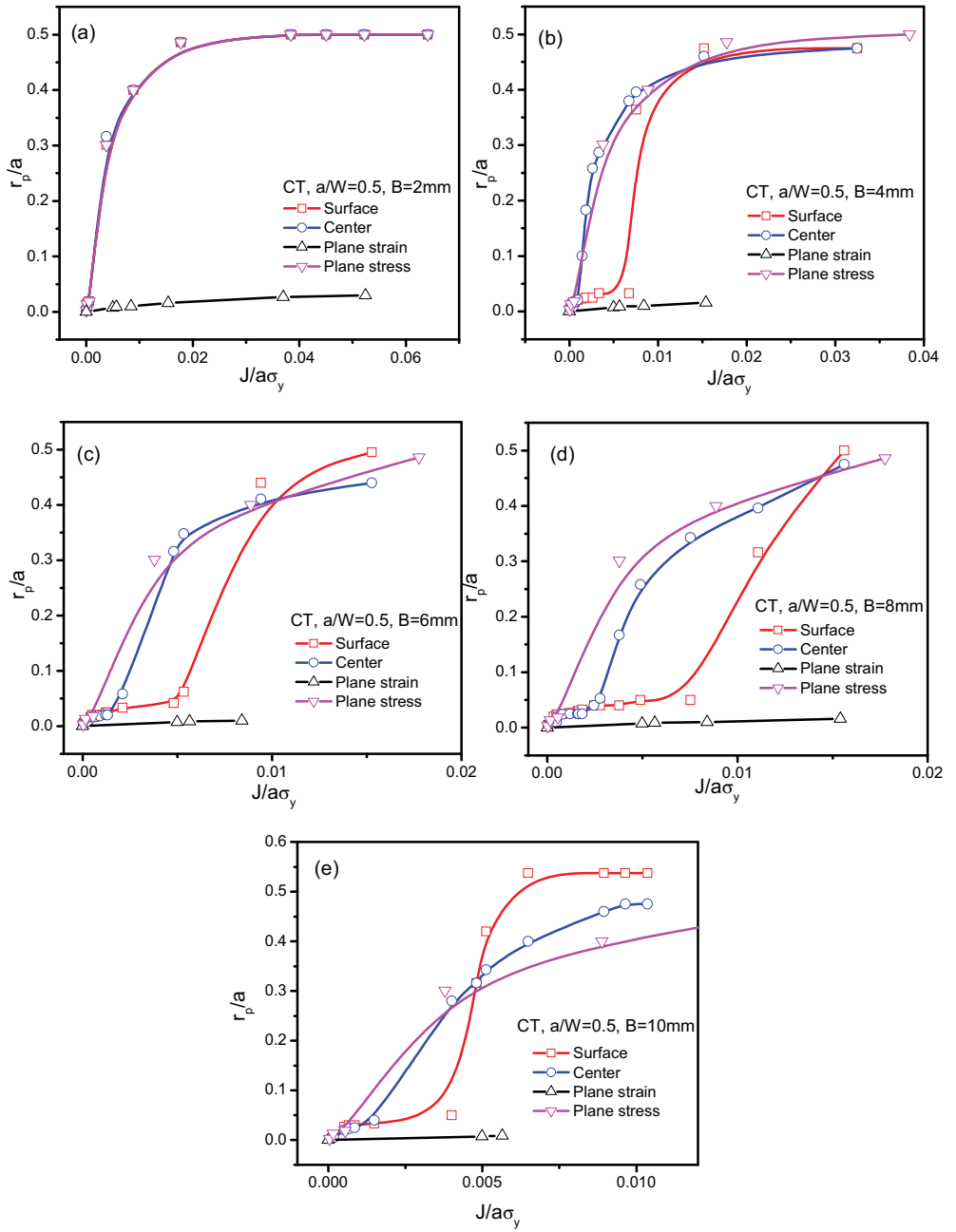

Fig.7 Variation of r_p/a vs. $J/a\sigma_y$ for various specimen thickness

To clearly understand the variation of PZS on surface and centre, for various applied J_{av}, the difference in magnitude of normalized PZS (r_p/a) is computed as:

$$(r_p/a)_{diff} = (r_p/a)_{surface} - (r_p/a)_{centre} \quad (2)$$

The computed $(r_p/a)_{diff}$ for all magnitude of applied load are plotted against normalized J_{av} in Fig.8(a). This figure indicates that the magnitude of $(r_p/a)_{diff}$ is zero for significantly small and for higher magnitudes of normalized J_{av} indicating similar PZS along the specimen thickness. This result infers that the stress field approaches a state of plane strain, only when J_{av} becomes vanishing small and plane stress when it is higher, these values of J being specimen thickness dependent as shown in Fig.8(a). For clarity at lower magnitudes of normalized J, the Fig.8 (b) is plotted for lower values of normalized J. It is observed from this figure that for $J/a\sigma_y \leq 0.0009$, the $(r_p/a)_{diff} \cong 0$, which indicates the state of plane strain with highest crack-tip constraint. One can obtain the specimen dimensions for the J_{IC} test from the above relation, which can be used to estimate J_{IC} independent of specimen thickness. But use of the restriction mentioned above results in large specimen thickness than the one presentably recommended in the ASTM standard [7]. The 3D PZS results obtained in this study point out towards the need of further investigation on some modification on size requirement of J_{IC} test.

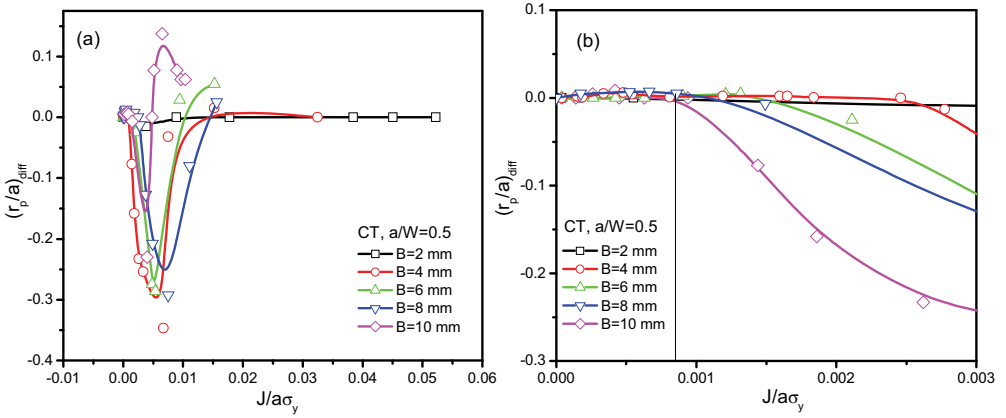

Fig.8 variation of $(r_p/a)_{diff}$ vs. $J/a\sigma_y$ (a) all applied loads (b) lower applied

Summary and Conclusions

In this investigation the shape and size of the crack-tip plastic zone in a CT specimen has been studied by elastic-plastic FE analysis to elucidate the constraint effects on fracture. Following are the conclusions made from the present analysis:

(a) the shape of the 3D plastic zone obtained by elastic-plastic FE analysis does not correspond to classic "*dog-bone*" shape,
(b) the maximum plastic zone size is found to occur at the centre of the specimen, in contrary to conventional shape, indicating a significant change in the shape of plastic zone,
(c) plane stress conditions are found to exist at the crack-tip for specimens with $B/W \leq 0.1$, for $0.1 \geq B/W \leq 0.5$, plane strain crack-tip condition as expected is not observed.
(d) due to varied shape of PZS in 3D, the fracture analysis can not be controlled by a parameter defined under plane strain condition only.
(e) modification with respect to the minimum size requirement of J_{IC} test specimen may be necessary.

References

[1] H. J. Schinder: Facta Universities, Mechanics, Automatic control and robotics, vol. 3, 613-622 (2003)

[2] H. Yuan and W. Brocks: J. Mech. Phys. Solids, vol. 46, 219-249 (1998)

[3] C. Betegon and J. W. Hancock: J. Appl. Mech. Trans ASME, vol. 58, 104-116. (1991).

[4] N. P. O'Dowd, and C. F. Shih: J. Mech. Phys. Solids., vol. 39, 989-1015(1991)

[5] Z. D. Fernandez, J. F. Kalthoff, C.A. Fernandez , J. Grasa and M. Doblare: ECF 15 (2004)

[6] A. G. Herrea, J. G. Manrique, A. Cordero and J. Zapetero: Key Engineering Materials, vol. 324-325, pp.555-558 (2006).

[7] ASTM E813-87 (1994). Standard test method for J_{IC}, A measure of fracture toughness. Am. Soc. Test. Mats. (Philadelphia

[8] ABAQUS (2005) User's Manual, Version 6.5, Hibbitt, Karlsson and Sorensen Inc.

[9] Y.Kim, X.K.Zhu and Y.J.Chao: Engineering Fracture Mechanics, vol. 68, 895-914, (2001)

[10] S.Coutin, C.Gardin, G.Bezine, H.Ben Hadj Hamouda: Engineering Fracture Mechanics, vol. 72, 2174-2185, (2005)

[11] S. K. Kudari, Ph.D Thesis, IIT, Kharagpur, India (2004)

[12] S. K. Kudari, B. Maiti and K. K. Ray: J of Strain Analysis, vol. 42, 121-132 (2007)

[13] A. H. Priest: J. Strain Analysis, vol.10,.225-232, (1975)

[14] K. G. Kodancha and S. K. Kudari: Accepted article, ECF 17 (2008)

[15] G. M. Zadeh, K. D. Hardtke, P. Wossidlo, K. Wobst: Nuclear Engineering and Design, 157, 111-121, (1995)

[16] H. Rajaram, S. Socrate, D.M. Parks: Engineering Fracture Mechanics, vol. 66, 455-482, (2000)

[17] S. Roychoudhury and R. H. Dodds Jr.: Engineering Fracture Mechanics, vol. 70 2363–2383, (2003)

[18] ASTM E399-83 (1994). Standard test method for plane strain fracture toughness for metallic materials, Am. Soc. Test. Mats. (Philadelphia.)